

Diffraction of an Arbitrary Uniform Complex-Source Beam by a Perfectly Conducting Wedge

Ludger Klinkenbusch and Giuliano Manara

Abstract – This article deals with a new spherical-multipole solution for the diffraction of an arbitrarily incident uniform complex-source beam (UCSB) by a perfectly conducting wedge. The well-known solution in spherical coordinates for an incident field produced by a Hertzian dipole is extended by the definition of complex-valued coordinates of the dipole and by using only spherical Bessel functions of the first kind for describing the radial dependencies. The finally obtained scattered far field shows a maximum in directions lying on the Keller cone but also cross-polarized components. The occurrence of cross-polar components was already observed in a previous asymptotic solution concerning the three-dimensional diffraction of an inhomogeneous plane wave by a perfectly conducting wedge. Consequently, among other things, the availability of the present rigorous solution opens the way to thoroughly analyze the scattering phenomena induced by the incident UCSB or its plane-wave spectrum at the edge of the wedge. Moreover, it will be possible to systematically check the validity and accuracy of different asymptotic methods when the observation point is placed either relatively close to or far from the edge.

1. Introduction

The scattering and diffraction of electromagnetic waves by a perfectly conducting wedge including the half plane counts to the classical canonical problems. A comprehensive overview on this subject that also includes the corresponding scalar (acoustic) boundary-value problems and different types of incident fields (plane wave, point source, dipole source) can be found in [1]. Further work, particularly regarding the computational calculation of the needed Ferrers functions of the first kind (associated Legendre functions of the first kind on the cut; see [2], chap. 14), has been presented in [3]. Particularly, the solution for an incident field produced by an arbitrarily oriented Hertzian dipole is of interest, as it will be extended in this work to a uniform complex-source beam (UCSB), representing a Gaussian beam-like incident field by just defining a complex-valued coordinate. Preliminary work on this subject with results for the acoustic case has been presented in [4] and [5].

The present work deals with the electromagnetic case, which is described here in a compact form strictly

using \vec{M} and \vec{N} function notations [6] and a field representation that follows from the corresponding dyadic Green's function [7]. Numerical results include total near fields and scattered far fields. In addition, the numerical calculation of the Ferrers functions is explained. Parts of this article's content have been presented in [8].

2. Formulation of the Three-Dimensional Boundary-Value Problem

The geometry of the electromagnetic boundary-value problem is depicted in Figure 1. Using spherical coordinates r, ϑ, φ with the z -axis as the polar axis, the two faces of a perfectly electrically conducting (PEC) wedge are given by $\varphi = 0$ and $\varphi = \beta$, respectively. Consequently, the edge of the wedge coincides with the z -axis. We are looking for the electromagnetic field at all r, ϑ, φ with $0 \leq r$, $0 \leq \vartheta \leq \pi$, $0 \leq \varphi \leq \beta \leq 2\pi$. The incident field is given by an arbitrary electromagnetic UCSB [9] with its waist at \vec{r}' and with Rayleigh length b , traveling in the direction of \vec{b} toward the origin ($r = 0$) on the z -axis.

3. Solution of the Boundary-Value Problem

We start from the scalar solutions $\Phi_{\text{h}}^{\text{s}}$ of the Helmholtz equation for an incident UCSB of amplitude A illuminating an acoustically soft (s) or hard (h) wedge [1, 3, 5],

$$\Phi_{\text{h}}^{\text{s}} = \frac{\beta}{2\pi} \sum_{n=0}^{\infty} \sum_{m=0}^{\infty} a_{nm}^{\text{h}} j_{n+\tau_m}^{\text{s}}(kr) \mathbf{P}_{n+\tau_m}^{-\tau_m}(\cos \vartheta) \frac{\sin(\tau_m \varphi)}{\cos(\tau_m \varphi)} \quad (1)$$

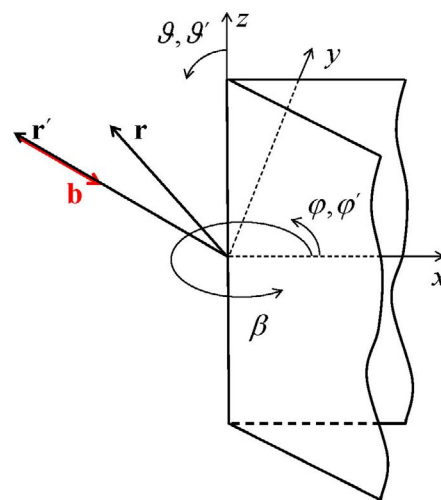


Figure 1. Description of the boundary-value problem.

Manuscript received 20 December 2021.

Ludger Klinkenbusch is with Kiel University, Kaiserstrasse 2, D-24143 Kiel, Germany; e-mail: klinkenbusch@tf.uni-kiel.de.

Giuliano Manara is with the University of Pisa, Via G. Caruso 16, I-56122 Pisa, Italy; e-mail: giuliano.manara@unipi.it.

$$a_{nm}^s = A\gamma_{nm}j_{n+\tau_m}(\kappa r_c)\mathbf{P}_{n+\tau_m}^{-\tau_m}(\cos\vartheta_c)\frac{\sin(\tau_m\varphi_c)}{\cos(\tau_m\varphi_c)} \quad (2)$$

where

$$\tau_m = \frac{m\pi}{\beta} \quad (3)$$

$$\gamma_{nm} = \frac{2}{\varepsilon_m\beta}\frac{\Gamma(n+2\tau_m+1)}{n!}[2(n+\tau_m)+1] \quad (4)$$

$$\varepsilon_m = \begin{cases} 2 & n=0 \\ 1 & n=1,2,\dots \end{cases} \quad (5)$$

In (1)–(5), j_ν denotes a spherical Bessel function of the first kind of order ν , related to Bessel functions of the first kind J_ν by $j_\nu(x) = \sqrt{\frac{\pi}{2x}}J_{\nu+1/2}(x)$; κ is the wave number; \mathbf{P}_ν^μ is a Ferrers function of the first kind (also known as an associated Legendre function of the first kind *on the cut*) of degree ν and order μ ; and $\Gamma(x)$ represents a gamma function. The complex source coordinate \vec{r}_c is defined by

$$\vec{r}_c = \vec{r}' - j\vec{b}, \quad (6)$$

where \vec{r}' is the location of the beam's waist while the direction and amount of \vec{b} represent the direction of the beam's propagation and the Rayleigh (focus) length, respectively. As has been shown [9], by just assigning a complex value to the radial coordinate according to $r_c = r' + jb$ while leaving both ϑ_c and φ_c real valued, we obtain a UCSB with its waist at \vec{r}' traveling toward the center of the coordinate system on the z -axis. Since we are using a UCSB, we are able to locate the waist (i.e., the area where the beam's wave front is nearly plane) of the incident beam almost directly on the z -axis, that is, at the area of interaction between the UCSB and the wedge.

Next, we define an odd $(^{(o)})$ and even $(^{(e)})$ normalized elementary scalar solution according to

$$\psi_{nm}^{(e)} = j_{n+\tau_m}(\kappa r)Y_{nm}^{(e)}(\vartheta, \varphi) \quad (7)$$

$$Y_{nm}^{(e)}(\vartheta, \varphi) = \sqrt{\gamma_{nm}}\mathbf{P}_{n+\tau_m}^{-\tau_m}(\cos\vartheta)\frac{\sin(\tau_m\varphi)}{\cos(\tau_m\varphi)} \quad (8)$$

and obtain for the odd and even vector spherical-multipole functions [6]

$$\begin{aligned} \vec{M}_{nm}^{(e)} &= (\vec{r} \times \vec{\nabla})\psi_{nm}^{(e)} \\ &= j_{n+\tau_m}(\kappa r)\vec{m}_{nm}^{(e)}(\vartheta, \varphi) \end{aligned} \quad (9)$$

$$\begin{aligned} \vec{N}_{nm}^{(e)} &= \frac{1}{\kappa}\left[\vec{\nabla} \times (\vec{r} \times \vec{\nabla})\right]\psi_{nm}^{(e)} \\ &= -\frac{j_{n+\tau_m}(\kappa r)}{\kappa r}(n+\tau_m)(n+\tau_m+1)Y_{nm}^{(e)}(\vartheta, \varphi)\hat{r} \\ &\quad - \frac{1}{\kappa r}\frac{d}{dr}[rj_{n+\tau_m}(\kappa r)]\vec{n}_{nm}^{(e)}(\vartheta, \varphi) \end{aligned} \quad (10)$$

Here, Z represents the wave impedance, while the odd and even transverse vector functions are defined by

$$\vec{m}_{nm}^{(o)}(\vartheta, \varphi) = -\frac{1}{\sin\vartheta}\frac{\partial Y_{nm}^{(e)}}{\partial\varphi}\hat{\vartheta} + \frac{\partial Y_{nm}^{(e)}}{\partial\vartheta}\hat{\varphi} \quad (11)$$

$$\vec{n}_{nm}^{(e)}(\vartheta, \varphi) = \frac{\partial Y_{nm}^{(e)}}{\partial\vartheta}\hat{\vartheta} + \frac{1}{\sin\vartheta}\frac{\partial Y_{nm}^{(e)}}{\partial\varphi}\hat{\varphi} \quad (12)$$

With these definitions and the standard formalism for deriving the dyadic Green's function [7], we obtain for the electromagnetic field in the presence of a PEC wedge, illuminated by a UCSB beam with amplitude and electric polarization given by the direction of the current moment \vec{c}_{el} [9], which is again defined at the complex coordinate \vec{r}_c , the vector spherical-multipole expansion

$$\vec{E}(\vec{r}) = \sum_{n=0}^{\infty}\sum_{m=0}^{\infty}\left[A_{nm}\vec{N}_{nm}^{(o)}(\vec{r}) + \frac{Z}{j}B_{nm}\vec{M}_{nm}^{(e)}(\vec{r})\right] \quad (13)$$

$$\vec{H}(\vec{r}) = \sum_{n=0}^{\infty}\sum_{m=0}^{\infty}\left[\frac{j}{Z}A_{nm}\vec{M}_{nm}^{(o)}(\vec{r}) + B_{nm}\vec{N}_{nm}^{(e)}(\vec{r})\right] \quad (14)$$

with the spherical-multipole amplitudes

$$A_{nm} = -\frac{\kappa^2 Z}{(n+\tau_m)(n+\tau_m+1)}\vec{N}_{nm}^{(o)}(\vec{r}_c) \cdot \vec{c}_{el} \quad (15)$$

$$B_{nm} = -\frac{j\kappa^2}{(n+\tau_m)(n+\tau_m+1)}\vec{M}_{nm}^{(e)}(\vec{r}_c) \cdot \vec{c}_{el}. \quad (16)$$

For the calculation of the radiated far field, we have to take into account that this has to satisfy the radiation condition. Only that part of the total field in (13)–(16) that is proportional to $e^{-jk_r r}/r$ for $r \rightarrow \infty$ forms the radiated field. Because of

$$j_\nu(\kappa r) = \frac{1}{2}\left[h_\nu^{(1)}(\kappa r) + h_\nu^{(2)}(\kappa r)\right] \quad (17)$$

and

$$\kappa r \gg 1 \rightarrow h_\nu^{(2)}(\kappa r) \cong j^{\nu+1}\frac{e^{-jk_r r}}{\kappa r}, \quad (18)$$

we thus obtain for the radiated far field

$$\begin{aligned} \vec{E}_\infty(\vec{r}) &= \frac{1}{2}\frac{e^{-jk_r r}}{\kappa r} \\ &\times \sum_{nm} A_{nm}j^{n+\tau_m}\vec{n}_{nm}^{(o)}(\vartheta, \varphi) + Z \sum_{nm} B_{nm}j^{n+\tau_m}\vec{m}_{nm}^{(e)}(\vartheta, \varphi) \end{aligned} \quad (19)$$

with the multipole amplitudes given by (15) and (16). For the scattered far field, we simply subtract from (19) the radiated far field of the corresponding UCSB in the free space.

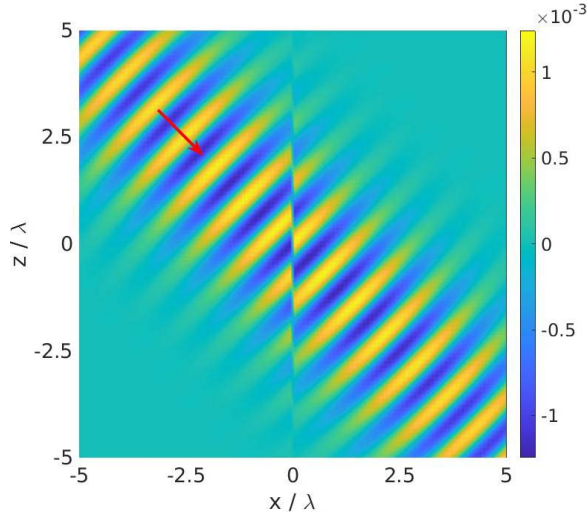


Figure 2. Normalized E_φ -component of a UCSB electrically polarized in the y -direction and incident on a half plane located in the xz -plane for $x > 0$. Waist at $r' = 0.001\lambda$, $\vartheta' = 45^\circ$, $\varphi' = 180^\circ$; Rayleigh length: $b = 10\lambda$.

4. Numerical Evaluation

We start with a UCSB that is incident on a PEC half plane ($\beta = 360^\circ$). The waist of the UCSB is located at $r' = 0.001\lambda$, $\vartheta' = 45^\circ$, $\varphi' = 180^\circ$, while the UCSB is traveling toward the origin with a Rayleigh length of $b = 10\lambda$.

Figure 2 shows the normalized total E_φ -component in the xz -plane. Actually, the incident field is undisturbed by the half plane because it is normally polarized with respect to it. The 180° change of the phase at $x = 0$ is due to the definition of the φ -coordinate.

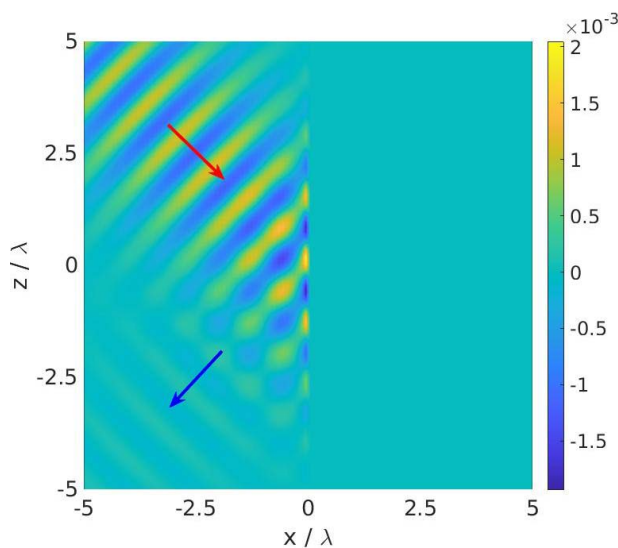


Figure 3. Normalized H_φ -component of a UCSB magnetically polarized in the y -direction and incident on a half plane located in the xz -plane for $x > 0$. For the other data, see Figure 2.

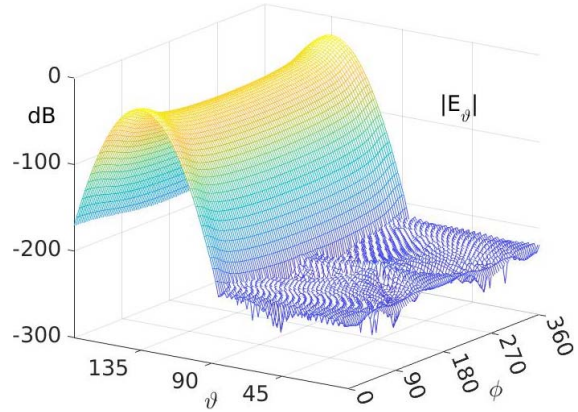


Figure 4. Normalized co-polarized scattered far field of a UCSB magnetically polarized in the y -direction and incident on a half plane located in the xz -plane for $x > 0$. For the other data, see Figure 2.

Figure 3 shows the normalized H_φ -component of a UCSB magnetically polarized in the y -direction, with other parameters as given in Figure 2. We observe that the normal magnetic field component vanishes on the PEC half plane and clearly identify the co-polarized part of the field diffracted by the half plane traveling in the direction of the Keller cone at $\vartheta = 135^\circ$ (blue arrow).

Figures 4 and 5 represent the co- and cross-polarized scattered far fields for the configuration described in Figure 3. We clearly observe that the maximum of the scattered far fields is along the Keller cone, that is, at $\vartheta = 135^\circ$, for both the co- and the cross-polarized fields. Such an appearance of a cross-polarized field does not occur in the case of an incident homogeneous plane wave but does, as has been shown in [10], for an incident inhomogeneous plane wave. Note that the plane-wave spectrum of a UCSB contains both homogeneous and inhomogeneous plane waves. If the waist of the incident UCSB is close to the edge and the beam impinges on the edge along its axis, this results in a dominant homogeneous part in the plane-wave spectrum. Correspondingly, this may justify why

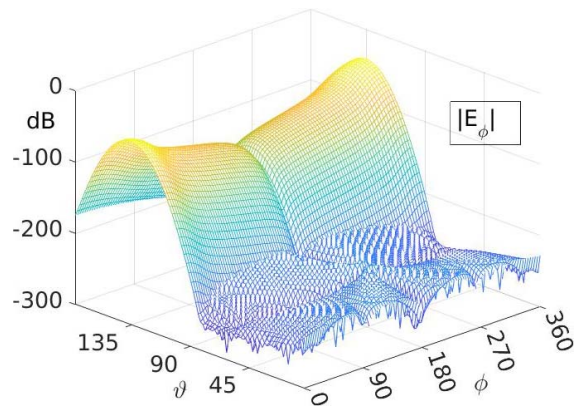


Figure 5. Normalized cross-polarized scattered far field of a UCSB magnetically polarized in the y -direction and incident on a half plane located in the xz -plane for $x > 0$. For the other data, see Figure 2.

in the present case the amplitude of the cross-polarized far field is much lower than that one of the co-polarized far field.

5. Conclusions

The diffraction of an arbitrary electromagnetic uniform complex-source beam by a perfectly conducting wedge has been investigated in a completely analytic way by means of the vector spherical-multipole expansion. Different from an incident homogeneous plane wave, the scattered far field consists of both a co- and a cross-polarized component. The next steps include the investigation of the exact origins of the cross-polarized far-field components, comparisons of the exact results of outcomes for the geometrical theory of diffraction and the uniform theory of diffraction in the far- and near-field regions of the scattering edge, and eventually the derivation of dyadic diffraction coefficients for the case of an incident uniform CSB.

Appendix: Numerical Evaluation of the Ferrers Functions of the First Kind

$P_{n+\tau_m}^{-\tau_m}(\cos \vartheta)$ for $n = 0, 1, 2, \dots$ and $\tau \in \mathbb{R}$

According to [4, eq. (14.5.18)], it holds for $n = 0$

$$P_{\tau_m}^{-\tau_m}(\cos \vartheta) = \frac{(\sin \vartheta)^{\tau_m}}{2^{\tau_m} \Gamma(\tau_m + 1)} \quad (20)$$

while from [4, eqs. (14.10.4) and (14.10.5)], we conclude for $n = 1$ that

$$P_{1+\tau_m}^{-\tau_m}(\cos \vartheta) = \cos \vartheta P_{\tau_m}^{-\tau_m}(\cos \vartheta) \quad (21)$$

For the remaining values of $n = 2, 3, \dots$, we exploit the recurrence relation [4, eq. (14.10.3)] and obtain

$$P_{n+2+\tau_m}^{-\tau_m}(\cos \vartheta) = \frac{1}{2\tau_m + n + 2} \left\{ [2(\tau_m + n) + 3] \cos \vartheta P_{n+1+\tau_m}^{-\tau_m}(\cos \vartheta) - (n + 1) P_{n+\tau_m}^{-\tau_m}(\cos \vartheta) \right\} \quad (22)$$

Finally, for the derivative of the Ferrers functions of the first kind, [4, eq. (14.10.4)] yields

$$\frac{dP_{n+\tau_m}^{-\tau_m}(\cos \vartheta)}{d\vartheta} = \frac{1}{\sin \vartheta} \left[(n + 2\tau_m + 1) P_{n+1+\tau_m}^{-\tau_m}(\cos \vartheta) - (n + 1 + \tau_m) \cos \vartheta P_{n+\tau_m}^{-\tau_m}(\cos \vartheta) \right] \quad (23)$$

6. References

1. J. J. Bowman, T. B. A. Senior, and P. L. E. Uslenghi (eds.), *Electromagnetic and Acoustic Scattering by Simple Shapes*, Revised Printing, New York, Hemisphere, 1998.
2. F. W. J. Olver et al. (eds.), *NIST Handbook of Mathematical Functions*, Cambridge, UK, Cambridge University Press, 2010.
3. O. M. Buyukdura, *Radiation From Sources and Scatterers Near the Edge of a Perfectly Conducting Wedge*, Ph.D. dissertation, Ohio State University, 1984.
4. S. Terranova, G. Manara, and L. Klinkenbusch, "A Physical Insight Into Complex-Source Beam Diffraction by a Wedge," Proceedings of the 2nd URSI Atlantic Radio Science Conference (AT-RASC), Gran Canaria, Spain, May 28–June 1, 2018.
5. L. Klinkenbusch, G. Manara, and S. Terranova, "3D Diffraction of a Uniform Complex-Source Beam by a PEC Wedge," Proceedings of the 2020 EuCAP European Conference on Antennas and Propagation, Copenhagen, Denmark, March 15–20, 2020.
6. J. A. Stratton, *Electromagnetic Theory*, New York, McGraw-Hill, 1941.
7. C. T. Tai, *Dyadic Green's Functions in Electromagnetic Theory*, Piscataway, NJ, IEEE Press, 1994.
8. G. Manara, L. Klinkenbusch, and S. Terranova, "3D Electromagnetic Scattering of a Complex-Source Beam by a PEC Wedge," URSI GASS 2021, Rome, Italy, August 28–September 4, 2021.
9. L. Klinkenbusch and H. Brüns, "Scattering and Diffraction of Scalar and Electromagnetic Waves Using Spherical-Multipole Analysis and Uniform Complex-Source Beams," in K. Kobayashi and P. D. Smith (eds.), *Advances in Mathematical Methods for Electromagnetics*, Raleigh, NC, SciTech Publishing, 2020.
10. R. G. Kouyoumjian, T. Celandroni, G. Manara, and P. Nepa, "Inhomogeneous Electromagnetic Plane Wave Diffraction by a Perfectly Conducting Wedge at Oblique incidence," *Radio Science*, **42**, RS6S06, 2007.